

PAPER • OPEN ACCESS

Infrared and Visual Image Fusion Based on NSST and Improved PCNN

To cite this article: Min Li *et al* 2018 *J. Phys.: Conf. Ser.* **1069** 012151

View the [article online](#) for updates and enhancements.

You may also like

- [Infrared and Visible Image Fusion Algorithm Based on Target Extraction](#)
Yumei Wang, Mingyi Zhang, Congyong Li et al.
- [An infrared and visible image fusion method based upon multi-scale and top-hat transforms](#)
Gui-Qing He, , Qi-Qi Zhang et al.
- [Blur Regional Features Based Infrared And Visible Image Fusion Using An Improved C3Net Model](#)
Zhao Xu, Gang Liu, Li Li Tang et al.



ECS
The
Electrochemical
Society
Advancing solid state &
electrochemical science & technology

DISCOVER
how sustainability
intersects with
electrochemistry & solid
state science research

Infrared and Visual Image Fusion Based on NSST and Improved PCNN

Min Li, Xianjie Yuan, Zhidan Luo and Xiaohua Qiu

Xi'an Research Institute of High Technology, Xi'an 710025 China

Abstract. Aiming at the difference characteristics between infrared image target information and visible images detail information, this paper proposed a novel infrared and visible images fusion algorithm based on Non-subsampled Shearlet Transform (NSST). Firstly we obtain the high and low frequency components by using the NSST multi-scale decomposition of the strictly registered source images. Secondly, the low frequency components are fused by using the modified spatial frequency as the external excitation of the PCNN, at the same time, the average gradient of low frequency components are used to adjust the link strength adaptively. Moreover, for the high frequency components, we present a self-adaptive fusion rule algorithm based on local area variance and local area average gradient. Finally, this paper uses the NSST inverse transform method to fuse low and high frequency components to obtain a fused image. Experimental results show that the proposed method of image fusion can effectively integrate important information in infrared and visible images, and the fusion effect is better than the general image fusion methods based on NSCT and NSST.

1. Introduction

Image fusion is taken from the same region of two or more images of different spectral and spatial details fused to a single image through a certain algorithm. Moreover, infrared and visible images fusion can comprehensively use the complementary characteristics of the infrared image background information and the details information of the visible images, which have important applications in the military[1] and civil fields, such as multi-source information mining, big data analysis, geological resources exploration, etc.

Based on previous fusion method in the dim light, background and target gray close, fusion image background detail information not fully exploiting problem, this paper proposes a fusion method of infrared and visible images based on NSST and improved PCNN. The algorithm firstly adopts NSST to decompose the infrared and visible images, which have been strictly matched, and obtains high and low frequency components, which high frequency components have the edge details of images and the display of texture information; other low frequency components contain the basic information of the image. Secondly, the modified spatial frequency of low frequency components are used as the external excitation of PCNN, at the same time, the average gradient of low frequency components are used to adaptively adjust the link strength of PCNN. Moreover, for the high frequency components, a self-adaptive fusion rule algorithm based on local area variance and local area average gradient is presented. Then, the fusion of low and high frequency components is reconstructed by NSST inverse transform. Finally, comparing the results of the proposed method with the results of five fusion methods based on the Curvelet transform[2], dual-tree complex wavelet transform (DTCWT), NSCT[3][4] transform, NSCT-PCNN[5] transform, and NSST[6][7][8] transform, which are typical multi-scale decomposition fusion methods. The superiority of this method is verified.



2. Image Fusion Strategy

2.1. Low Frequency Components Fusion Rule

After the NSST [9] [10], the low frequency components contain the basic information of the image, which is to remove the texture and the details of the thumbprint, so the fusion of low frequency components are essential. The adjacent domain energy extraction method as far as possible retains the important edge of source image, but weakens the edge information of lower brightness to some extent. Therefore, for low frequency components, the modified spatial frequency (MSF) that is good at describing the image gradient characteristics is used to stimulate PCNN neurons. Not only can better overcome the Gibbs phenomenon, but also more fully reflect the image details. The specific process is as follows:

2.1.1 Calculate the modified spatial frequency MSF^I . The spatial frequency (SF) uses the sliding window to select the low frequency components and calculates the gradient energy in the row and column directions. Low frequency components $C^I(i, j)$ are obtained by NSST decomposition. MSF^I definition is as follows:

$$MSF^I = \frac{1}{M \times N} \sum_{i=1}^M \sum_{j=1}^N (RF^I + CF^I + MDF^I + SDF^I) \quad (1)$$

In the Eq.(1), $I = (A, B, F)$ (A indicates infrared images, B indicates visible images, F represents fusion images), RF^I , CF^I , MDF^I and SDF^I respectively represent row frequency, column frequency, main pair angular frequency and pair angular frequency. M and N represent the size of the rectangular window of MSF^I . This paper selects the neighborhood region of 3×3 .

2.1.2 Calculate the adaptive link coefficients β_{ij}^I . The average gradient of the image represents the transformation of the gray value of the image. In addition, It can also represent details such as boundaries and textures. The mathematical expression of average gradient is as follows:

$$\bar{G}^I(i, j) = \frac{1}{(M-1)(N-1)} \sum_{i=1}^{M-1} \sum_{j=1}^{N-1} \{[(C^I(i+1, j) - C^I(i, j))^2 + (C^I(i, j+1) - C^I(i, j))^2] / 2\}^{1/2} \quad (2)$$

In the Eq.(2), $\bar{G}^I(i, j)$ denotes the average gradient in the local neighborhood of $M \times N$ at the (i, j) position. At this point, the link coefficient is defined as:

$$\beta_{ij}^I = \frac{1}{1 + \exp(-\bar{G}^I(i, j))} \quad (3)$$

According to the Eq.(3), β_{ij}^I reflect the change of gray value in the image window.

2.1.3 Calculate low Frequency Fusion Components.

1) The adaptive connection coefficient β_{ij}^I are determined by the method proposed above.

2) Perform initialization of PCNN model parameters. $L_{ij}(0) = U_{ij}(0) = Y_{ij}(0) = T_{ij}(0)$, Number of iterations $n = N_{\max}$.

3) Input MSF^I as incentives to enter the PCNN model. The final number of firings for the two source images are denoted as $T_{ij}^A(n)$ and $T_{ij}^B(n)$.

4) PCNN low frequency fusion is derived from Eq.(4).

$$C^F(i, j) = \begin{cases} C^A(i, j), & T_{ij}^A(n) \geq T_{ij}^B(n) \\ C^B(i, j), & \text{otherwise} \end{cases} \quad (4)$$

2.2. High Frequency Components Fusion Rule

After the decomposition of NSST, the high frequency components mainly correspond to the edge details of images and the display of texture information, which will directly affect the visual effect of the fusion image. The variance of local area reflects the intensity of the change of the regional components, and to some extent reflects the clarity of the image in the region. The local average gradient reflects details such as the boundary and texture of the region. Therefore, the high frequency components adopt adaptive weighting method based on local average gradient and local variance.

High frequency components $C_{s,d}^I(i, j)$ are obtained by NSST decomposition. $s = (2, \dots, k)$ represent image resolution scale, d indicates the number of directions on the s scale. The definition is as follows:

$$V_{s,d}^I(i, j) = \frac{1}{M \times N} \sum_{m=1}^M \sum_{n=1}^N [C_{s,d}^I(i+m, j+n) - \bar{C}_{s,d}^I(i, j)]^2 \quad (5)$$

$$\bar{G}_{s,d}^I(i, j) = \frac{1}{(M-1)(N-1)} \sum_{i=1}^{M-1} \sum_{j=1}^{N-1} \{ [(C_{s,d}^I(i+1, j) - C_{s,d}^I(i, j))^2 + (C_{s,d}^I(i, j+1) - C_{s,d}^I(i, j))^2] / 2 \}^{1/2} \quad (6)$$

The high frequency components of the fused image F is obtained by Eq.(7).

$$C_{s,d}^I(i, j) = \begin{cases} C_{s,d}^A(i, j) & V_{s,d}^A(i, j) > V_{s,d}^B(i, j) \text{ and } \bar{G}_{s,d}^A(i, j) > \bar{G}_{s,d}^B(i, j) \\ \omega_1 C_{s,d}^A(i, j) + \omega_2 C_{s,d}^B(i, j) & \text{otherwise} \\ C_{s,d}^B(i, j) & V_{s,d}^A(i, j) < V_{s,d}^B(i, j) \text{ and } \bar{G}_{s,d}^A(i, j) < \bar{G}_{s,d}^B(i, j) \end{cases} \quad (7)$$

The weight coefficients ω_1 and ω_2 are obtained from Eq.(8).

$$\begin{cases} \omega_1 = \frac{V_{s,d}^A(i, j)}{V_{s,d}^A(i, j) + V_{s,d}^B(i, j)} \\ \omega_2 = 1 - \omega_1 \end{cases} \quad (8)$$

2.3. Infrared and Visible Image Fusion Process.

In this paper, the image fusion process is shown in figure 1. Before fusion, the source image is strictly matched. The specific fusion steps are as follows:

1) The two source images A and B are decomposed by NSST to obtain corresponding low frequency components and high frequency components.

2) Apply the fusion rules proposed in this paper for low frequency components and high frequency components.

3) Finally, the fusion image is obtained by NSST inverse transform.

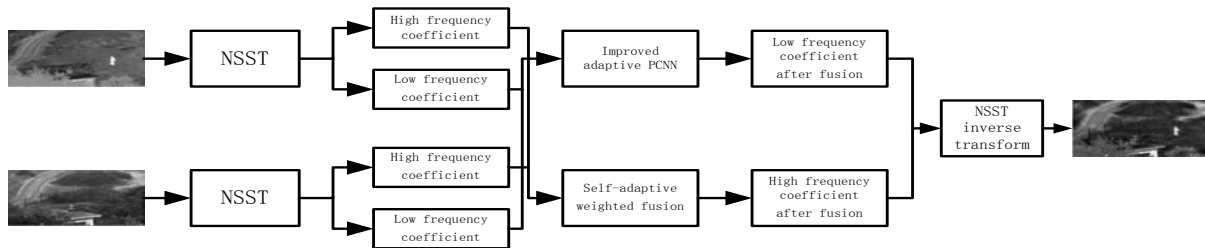


Figure 1. The method diagram of this paper

3. Experimental Results and Analysis.

In order to verify the validity of this algorithm, all experiments are conducted with Windows 7 operating system, CPU main frequency 3.20 GHz, memory 8.00 GB, and using platform Matlab R2014a for simulation. In this paper, the number of NSST decomposition layers is 4 layers, and the “maxflat” filter is used for multi-scale decomposition. The size and direction progression of the shear filter are respectively set to [30, 30, 36, 36] and [3, 3, 4, 4]. Adaptive PCNN model parameter settings: $W=[0.707,1,0.707;1,0,1;0.707,1,0.707]$, $V_{\theta} = 20$, $V_L = 1.0$, $\alpha_{\theta} = 0.1$, $\alpha_L = 1$, $N_{\max} = 200$.

Two groups of infrared and visible images are selected as source images; the size is 270 pixels \times 270 pixels. Select other five fusion methods to compare with this proposed method.

These five methods are respectively based on Curvelet transform, DTCWT, NSCT, NSCT-PCNN and NSST. As shown in figure 2 and figure 3.

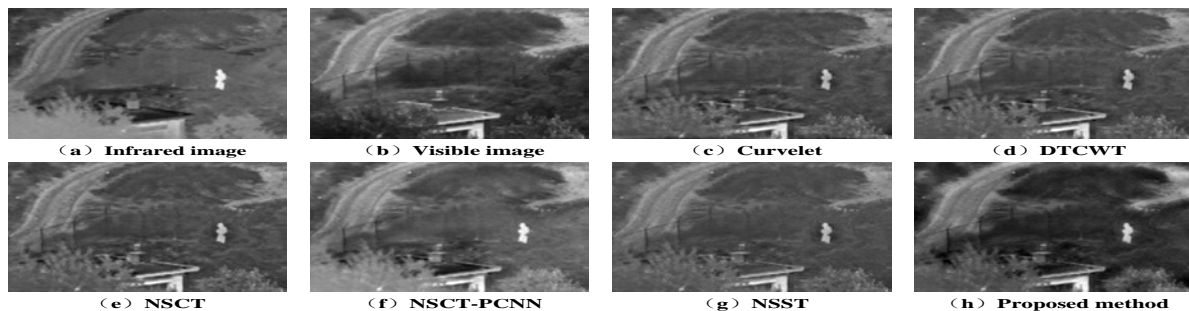


Figure 2. "UN Camp" fusion results

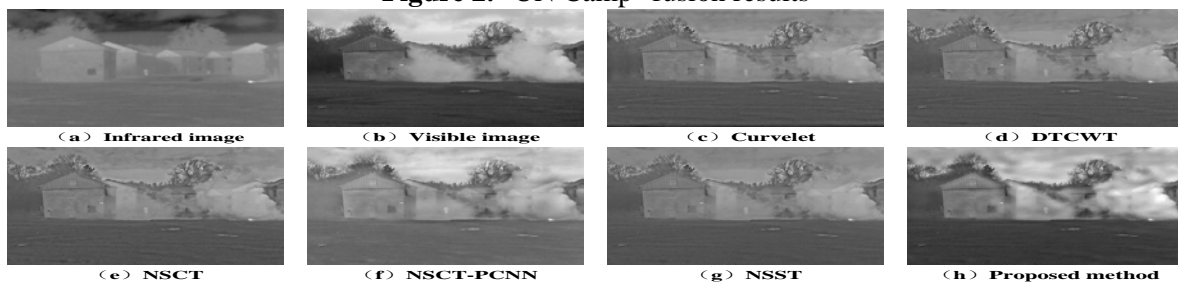


Figure 3. The second group of experimental results

Compare and analyze the fusion results in figure 2 and figure 3, The fused images based on Curvelet transform, dual-tree complex wavelet transform and NSCT transform have low contrast, low target and background, and overall dark. Use the NSCT-PCNN method, although the target is prominent, the background details of the fence, shrubs, trees and houses are lost. Based on the NSST method, the target is relatively dark and the contrast is low and not clear. The fusion image of the proposed algorithm is clear on the edge contour, the image texture and the source image are basically consistent, the character image features are the most significant. Overall visual perception is the best, and the texture of background details is better than other fusion algorithms. In order to evaluate the

experimental results objectively, the average gradient, spatial frequency, standard deviation, information entropy and correlation coefficient are used as objective evaluation criteria. Table 1 gives the quantitative evaluation results of the objective indicators of the above six fusion methods.

Table 1. Different fusion method indicators

Image group	Fusion method	Average gradient	Spatial frequency	Standard deviation	Information entropy	Correlation coefficient
“UN camp” group 1	Curvelet	5.7219	11.6383	27.3113	6.5552	0.4299
	DTCWT	5.6124	11.6060	26.6792	6.5019	0.4449
	NSCT	5.7879	11.7747	27.5368	6.5708	0.4850
	NSCT+PCNN	5.4352	11.0490	32.7306	6.9271	0.5531
	NSST	5.4312	11.1137	25.1133	6.4002	0.4783
	Proposed method	5.8083	11.7952	36.9376	6.9438	0.5357
Image of group 2	Curvelet	4.0007	10.7851	30.0317	6.5608	0.4513
	DTCWT	3.9408	10.7661	29.0826	6.4342	0.4595
	NSCT	4.0044	10.8076	29.2698	6.4454	0.4616
	NSCT+PCNN	3.7634	10.8763	38.8590	6.7837	0.2946
	NSST	3.8610	10.6756	28.8833	6.3799	0.4621
	Proposed method	4.0879	10.9392	53.7595	7.1072	0.4049

As can be seen from Table 1, among the five quantitative evaluation indexes of this method, except the correlation coefficient is slightly lower than NSCT-PCNN method or NSST method, all four other indicators are higher than the other five methods. It shows that the edge maintains high and the details of the image are more abundant. This shows that the overall performance of the proposed method is the best and consistent with the subjective visual effects.

4. Conclusions

This paper proposes a fusion method of infrared and visible images based on NSST and improved PCNN. This method makes full use of the characteristics of visible and infrared images, using the multi-resolution analysis of NSST to decompose images, the low frequency components adopt improved adaptive PCNN fusion rules, local frequency variance and local average gradient adaptive weighted average fusion rules for high frequency components. A large number of experimental results show that the proposed fusion method not only subjective visual effects, but also objective quantitative evaluation indicators is superior to Curvelet, DTCWT, NSCT, NSCT-PCNN, NSST. It is an effective infrared and visible images fusion method.

5. References

- [1] Liu J, Lei Y J, Xing Y Q Image fusion method based on improved NSST transform [J] 2017 *Control and Decision* **32** (2) 275 - 280
- [2] Wang H P, Liu Z Q, Fang X, et al Method for image fusion based on adaptive pulse coupled neural network in curvelet domain [J] 2016 *Journal of Optoelectronics Laser* **27**(4) 429 - 436
- [3] Chen M S Image fusion of visual and infrared image based on NSCT and compressed sensing[J] 2016 *Journal of Image & Graphics* **21**(1) 39 - 44
- [4] Ge W, Ji P, Zhao T Infrared image and visual image fusion algorithm based on NSCT and improved weight average [C] 2016 *The 6th International Conference on Intelligent Systems Design and Engineering Applications, IEEE* 456-459
- [5] Hao A Z, Zheng C Multi-sensor image fusion based on NSCT-PCNN transform [J] 2014 *Science Technology and Engineering* **14**(1) 45 - 48
- [6] Geng P, Wang Z Y, Zhang Z G, et al Image fusion by pulse couple neural network with shearlet [J] 2012 *Optical Engineering* **51**(6) 1-7
- [7] Shi Z, ZHANG Z, YUE Y G Adaptive image fusion algorithm based on shearlet transform [J] 2013 *Acta Photonica Sinica* **42**(1) 115 - 120

- [8] Miao Q, Shi C, Xu P, et al A novel algorithm of image fusion using shearlets [J] 2011 *Optics Communications* **284** (6) 1540 - 47
- [9] Liao Y, Huang W L, Shang L, et al Image fusion based on Shearlet and improved PCNN [J] 2015 *Computer Engineering and Applications* **50** (2) 142 - 146
- [10] Ge W, Ji P C, Zhao T C Infrared and visible image fusion based on NSST and CS [J] 2016 *Laser and Infrared* **46** (4) 502 - 506